A new binary encoding algorithm for the integration of hyperspectral data and DSM

Huan XIE
Tongji University, Department of Surveying and Geoinformatics, Shanghai, P.R. China, mailto:xiehuantj@gmail.com

Peter Lohmann
Leibniz University of Hannover, Institute of Photogrammetry and GeoInformation, Hannover, Germany, mailto:lohmann@ipi.uni-hannover.de

Keywords: Hyperspectral, DSM, binary encoding, classification, integration

ABSTRACT: A new binary encoding algorithm for the integration of hyperspectral data and DSM is proposed in this paper. If the hyperspectral data consists of L spectral channels, the ordinary binary spectral encoding method represents the spectral amplitude and the spectral slope with a 2L-bit binary code vector. Usually the Hamming distance is chosen as the similarity measure to determine the spectral signature matches.

Thinking that multi-source data may enhance the comprehension of images, we therefore attempt to integrate the spectral, shape and height information of remote sensing data of the same area by a modification of the binary encoding spectral matching method.

Several processing steps are required before the integration. First, segments have to be established. The ground objects were derived from DSM and ground segments were established using HyMap image by an edge-based segmentation algorithm. Second, the mean spectrum was selected as the representative spectrum of the segment. After that, six shape descriptors, area, asymmetry, elliptic fit, rectangular fit, the ratio of length to width, and compactness, were calculated for each segments and transformed to binary codes. The relative heights derived from DSM were converted to binary codes too.

The test data set covers an area in Oberpfaffenhofen, Germany. We tested the proposed method and the results show that the modified binary encoding classification is beneficial especially for discriminating similar spectral signatures.

1 INTRODUCTION

Binary spectral encoding is well known as a simple, effective, and with small computational load hyperspectral analysis method in classification, searching of similar spectra and identifying mineral components (Mazer *et al.* 1988). Although this method is frequently used and offers good performance, it still has some weaknesses. Due to the high spatial resolution of modern hyperspectral sensors and because this method mainly operates on pixels, the efficiency sometimes is low. Nowadays, with the rapid development of advanced remote sensor technologies with increasing spatial resolution, object-based data processing methods are more frequently applied. This paper therefore attempts to integrate an object based approach with traditional hyperspectral processing methods to support and enhance the information extraction from remote sensing data.

Several processing steps have to be performed before the integration. First segments have to be established. In this paper, an edge-based segmentation algorithm and the Full Lambda-Schedule algorithm (Robinson *et al.* 2002) are employed to partition the data spatially and merge adjacent segments, respectively. As one segment then is composed from many pixels, a method to choose a representative spectrum for this specific object has to be found. Here, because of simplicity, the mean spectrum was used as representative spectrum for each segment. The most important task then is, to find a way to integrate shape and height information with binary coding, like it is done with the spectral information. Several shape description measures, *e.g.*, area, compactness, will be discussed.

Following this introduction, a short description of the study area is given. Then data processing and binary encoding methods used in this paper, especially the representation of different kinds of features (spectral, shape and height information) with binary coding is presented as well as the computation of the signature distances. Practical tests, illustrating the proposed methods are presented and finally some conclusions are drawn at the end.

2 METHODS

2.1 *Study area*

The study area Oberpfaffenhofen is located in the south of Germany. The available digital surface model of this region has a spatial spacing of 0.5 meters. The Hymap data of this area was captured at 13:00, June 7, 2004 at a fight altitude of 2580 meters above sea level, and a flight direction from south to north (3.6°). This data has a ground resolution of 4 meters and 126 channels. Technical details of the HyMap sensor can be found in the reference (Cocks *et al.* 1998).

2.2 *Flowchart*

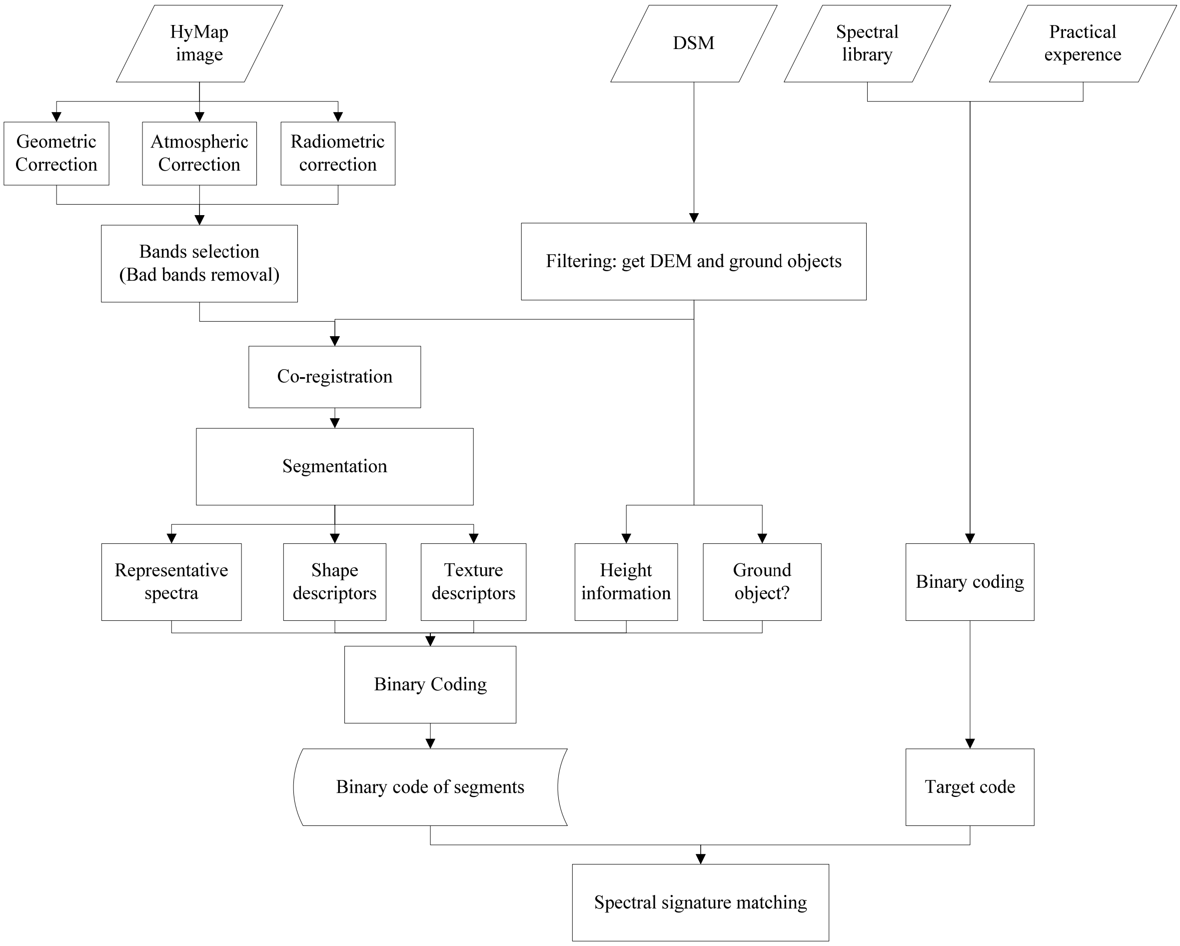

Figure. 1 Project flow chart

2.3 *Segmentation*

An edge-based segmentation algorithm is used for the segmentation and the Full Lambda-Schedule algorithm created by Robinson *et al.* (2002) is employed in the subsequent merge of adjacent segments. The segmentation and segment merging of the HyMap image was processed by ENVI Zoom module. This algorithm iteratively merges adjacent segments based on a combination of spectral and spatial information. Merging proceeds if the algorithm finds a pair of adjacent regions, *i* and *j*, such that merging cost $t_{i,j}$ is less than a defined threshold lambda value, which ranges from 0.0 to 100.0:

$$t_{i,j} = \frac{\dfrac{|O_i| \cdot |O_j|}{|O_i| + |O_j|} \cdot \|u_i - u_j\|^2}{length(\partial(O_i, O_j))} \tag{1}$$

Where
O_i is region *i* of the image
$|O_i|$ is the area of region *i*
u_i is the pixel mean value in region *i*
u_j is the pixel mean value in region *j*
$\|u_i - u_j\|$ is the Euclidean distance between the spectral values of regions *i* and *j*
$length(\partial(O_i, O_j))$ is the length of the common boundary of O_i and O_j
The lambda value we chose here is 88.0.

2.4 *Binary encoding for segments*

The binary code of a segment in our research is constructed by a 285-bit long code, which consists of three parts, i.e., spectral, shape and height. The spectral amplitude and slope are represented by 252 codes Y_{ij}, the shape of the segment is represented by 30 codes $\overrightarrow{Z_{ij}}$, and the relative height of a segment is represented by 3 codes. Specific explanations for these codes can be found in following contents.

2.4.1 *Spectra information*

Layer mean values are calculated from the layer values of all n pixels forming an image object.

In spectral binary encoding method, a single spatial resolution element of the image (pixel) is denoted by an L-dimensional vector,

$$\vec{X}_{ij} = \left[X_{ij}(1), X_{ij}(2), \ldots, X_{ij}(l), \ldots, X_{ij}(L) \right]^T \tag{2}$$

where L is the number of spectral channels, and the indices (i, j) refer to the spatial location of the pixel within a given scene. Defining the scalar quantity ν_{ij} as the spectral mean of pixel (i, j),

$$\nu_{ij} = \left[\frac{1}{L} \right] \sum_{l=1}^{L} X_{ij}(l) \tag{3}$$

an L-bit binary code vector $\overrightarrow{Y_{ij}^a}$ is constructed from

$$\overrightarrow{Y_{ij}^a} = H\left\{ \vec{X}_{ij} - \nu_{ij} \right\} \tag{4}$$

where $H(\nu)$ is the unit step operator defined by

$$H(\nu) = \begin{cases} 1, & \nu \geq 0, \\ 0, & \nu < 0. \end{cases} \tag{5}$$

The constructed vector is a binary representation of spectral amplitude; however, considerable information is contained in the local slope at each measured wavelength. Therefore, an additional L-bit code vector $\overrightarrow{Y_{ij}^b}$ is constructed from

$$Y_{ij}^{b} = \begin{cases} 1, \left[X_{ij}(l+1) - X_{ij}(l-1) \right] \geq 0, \\ 0, \left[X_{ij}(l+1) - X_{ij}(l-1) \right] < 0, \end{cases} \quad l = 1, 2, \ldots, L. \tag{6}$$

Here $X_{ij}(0)=X_{ij}(L)$, $X_{ij}(L+1)= X_{ij}(1)$, these two code vectors are then concatenated to form a single, 2L-bit code vector Y_{ij} , which is taken to be the binary code word representing the spectrum of pixel (i, j).

The calculation for the spectral binary codes was realized by IDL/ENVI programming.

2.4.2 *Shape information*

The value of shape attribute can be either computed by professional software, *e.g.*, eCongnition, or collected by IDL/ENVI programmes. The shape attributes of a segment are represented by a 30 bit long binary code, including the information of area, asymmetry, elliptic fit, rectangular fit, the ratio of length to width, and compactness. Each shape descriptor is represented by a 5-bit long binary code.

Area

In nongeoreferenced data the area of a single pixel is 1. Consequently, the area of an image object is the number of pixels forming it. If the image data is georeferenced, the area of an image object is the true area covered by one pixel times the number of pixels forming the image objects.

The areas of the segments in our study area ranges from 16 square meters to 1162000 square meters (from 1 to 72625 pixels), according to the histogram of the areas of the segments. We separate the segments into 5 cases by their areas. Each case covers approximately 20 percents of the histogram area. According to thresholds, the area of the segment can be expressed by a 5-bit long binary code. Such as 01000, means the area of this segment ranges from 20 to 40 percent in the histogram.

Asymmetry

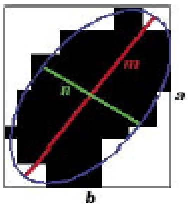

Figure. 2 The outer bounding box and the ellipse of a image object

The lengthier an image object, the more asymmetric it is. For an image object, an ellipse is approximated which can be expressed by the ratio of the lengths of minor and major axes of this ellipse (see equation 7 and Figure 2).

The feature value increases with the asymmetry, and the asymmetry value for a segment ranges from zero to one.

$$\kappa = 1 - \frac{n}{m} \tag{7}$$

According to the histogram, like the binary description of the area, the Asymmetry value of a segment can be expressed by a 5-bit long binary code.

Compactness

In eCognition, compactness is defined as the ratio of the area of a polygon to the area of a circle with the same perimeter. The following formula is used to calculate the compactness of the selected polygon. The compactness of a segment ranges from zero to one and a circle has the highest compactness value.

$$compactness = \frac{4 \cdot \pi \cdot Area}{Perimeter^2} \tag{8}$$

According to the histogram, like the binary description of the area, the Compactness value of a segment is expressed by a 5-bit long binary code in our research.

Elliptic Fit

As a first step in the calculation of the elliptic fit is the creation of an ellipse with the same area as the considered object. In the calculation of the ellipse also the proportion of the length to the width of the Object is regarded. After this step the area of the object outside the ellipse is compared with the area inside the ellipse that is not filled out with the object. While 0 means no fit, 1 stands for a complete fitting object.

According to the histogram, like the binary description of the area, the Elliptic Fit value of a segment can be expressed by a 5-bit long binary code.

Rectangular fit

A first step in the calculation of the rectangular fit is the creation of a rectangle with the same area as the considered object. In the calculation of the rectangle also the proportion of the length to the width of the object in regarded. After this step the area of the object outside the rectangle is compared with the area inside the rectangle, which is not filled out with the object. While 0 means no fit, 1 stands for a complete fitting object.

According to the histogram, like the binary description of the area, the Rectangular Fit value of a segment can be expressed by a 5-bit long binary code.

Length/width ratio

There are two ways to compute the length/width ratio of an image object.

The ratio length/width is identical to the ratio of the eigenvalues of the covariance matrix of the image object with the larger eigenvalue being the numerator of the fraction.

$$\gamma = \frac{l}{w} = \frac{eig_1(S)}{eig_2(S)},\ eig_1(S) > eig_2(S) \tag{9}$$

Or the ratio length/width can also be approximated using the bounding box.

$$\gamma = \frac{l}{w} = \frac{a^2 + ((1-f)\cdot b)^2}{A} \tag{10}$$

a is the length of the bounding box of the segment, *b* is the width of the bounding box, f is the degree of filling, which is the area *A* covered by the image object divided by the total area *a* * *b* of the bounding box.

We use both methods for the calculation and takes the smaller of both results as the feature value. The minimum value of the Length/width is one.

According to the histogram, like the binary description of the area, the Length/width value of a segment can be expressed by a 5-bit long binary code.

The values of shape descriptors were calculated using Definiens eCongnition and ESRI's ArcGIS software, the binary encoding for those shape descriptors were realized by IDL/ENVI programming.

2.4.3 *Height information*

Using filtering methods, we roughly separated ground objects from DSM, and the binary code of height is determined by the relative height of segments.

According to the practical height of ground objects, we separate the relative height of the segments into three cases: height less than 1.5 meters, height greater than 1.5 meters but less than 5meters, and height greater than 5 meters.

The relative height information were derived from the DSM data using the Surfer 8 software of the Golden Software Inc., the binary codes were calculated by IDL/ENVI programming.

2.5 *Target codes*

According to the situation of our study area, several codes for certain targets have been set up. According to the land use, we selected the classed Building, Transport, Vacant, Green belts, Agriculture, Forestry, Water, Grassland, and Outdoor recreation. More classes, especially different types of vegetation, can be set up following in-situ measurement and investigations. Corresponding codes were created for every target for further signature matching.

Several assumptions have been met before coding certain targets, which will be verified by *in-situ* investigation in future. These assumptions are:

1. The residential, industry and commerce areas are covered by buildings. The spectrum of the building varies depending on the materials and the vegetation cover of the roof.
2. Transport areas have similar spectrum like Vacant. The Transport and Vacant are separated by the shape and the ratio of length to width.
3. Green belts have a similar spectrum compared to Forestry, but the areas of Green belts are smaller than those of forestry.
4. Agriculture land is classified into several categories according to its status.

The principles of setting the target code are listed in Table 1.

Table. 1 The classification targets and their features

Classes	Number of spectral samples	Bin(s) of histogram						
		Shape						Height
	Spectrum	Area	Asymmetry	Compactness	Elliptic Fit	Length/width	Rectangular Fit	Relative Height
Building	10			4,5				2,3
Transport	5			1-3		5		1
Vacant	5			4,5			4,5	1
Green Belts	4	1						1
Agriculture	14*	2-5						1
Forestry	3	2-5						1
Grassland	2							1
Outdoor recreation	3	1,2				1-3		1

* Six types of land are included in 14 samples of Agriculture

Column 1 lists the Land use type we used in our test. Column 2 lists the corresponding number of spectral samples. Column 3 to 8 lists the requirements for shape descriptors. Column 9 lists the properties of height. Blanks in column 3 to 8 mean that there are no corresponding requirements for this attribute.

The spectral binary codes of targets were represented by 2*126 bit long codes, following the same way with the segment encoding.

Comparing to the codes of spectrum, the codes for the shape and height of targets are handled in a different way. Take the area of forestry for example, the area of forestry ranged from Area 2 to Area 5, the binary code for the area of forestry is 01111. The binary code for the blanks in column 3 to 8 is 00000.

2.6 *Signature matching*

The similarity measure used to determine spectral signature matches is the Hamming distance (Viterbi and Omura, 1979), which is computed from

$$D_h(\overrightarrow{Y_{ij}}, \overrightarrow{Y_{mn}}) = \sum_{l=1}^{2\times L} Y_{ij}(l)(XOR)Y_{mn}(l) \quad \in \{0,\cdots,252\} \tag{11}$$

which is seen to be just a 2L sum of bit-wise exclusive-OR operations. In the actual implementation of this algorithm, Hamming distances D_h^a and D_h^b are computed separately for the two components of the vectors $\overrightarrow{Y_{ij}}$ and $\overrightarrow{Y_{mn}}$ which are being compared. This gives the user some additional flexibility in weighting the importance of amplitude and slope information.

Different from the spectral data, the operator used in the similarity evaluation of shape and height descriptors is the bit-wise AND operation, which is more like a mask operation, which is computed from

$$D_a(\overrightarrow{Z_{ij}}, \overrightarrow{Z_{mn}}) = \sum_{l=1}^{33} Z_{ij}(l)(AND)Z_{mn}(l) \quad \in \{0,\cdots,6\} \tag{12}$$

This distance is more like a mask operation, in our research, only 1 or 0 will be shown in the results of calculation.

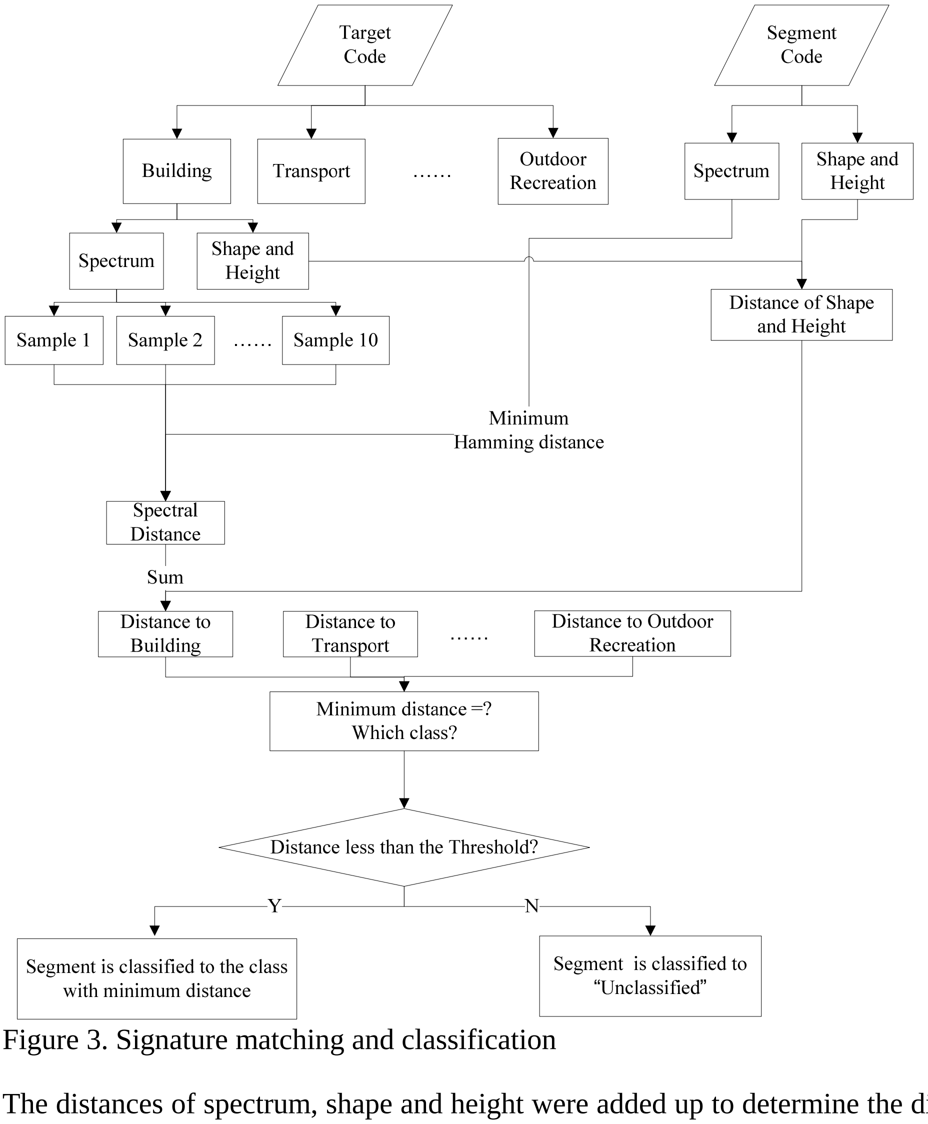

Figure 3. Signature matching and classification

The distances of spectrum, shape and height were added up to determine the distance to the targets. Since perfect matches rarely occur with real data, allowance for natural variability is made by specifying a threshold distance of acceptance, $\overline{d}$, such that

$$[\overrightarrow{Y_{ij}}, \overrightarrow{Z_{ij}}] \equiv [\overrightarrow{Y_{mn}}, \overrightarrow{Z_{mn}}] \ \ if \ \ D_h + D_a \leq \overline{d} \tag{13}$$

Or, if no threshold is set and several target classes are given, the minimum distance between the segment and all class targets is chosen as the distance of acceptance of this segment.

The specific procedure for signature matching and classification is shown in Figure 3. For one segment, the distance with all samples will first be calculated and the minimum distance *i* and the class *j* with the minimum distance will be recorded. If the distance *i* is less than the threshold, the segment will be assign to class j, or the segment will be assign to the class "Unclassified".

3 RESULTS

To compare the classification results, binary encoding classification were used on the raw HyMap data and the segment regional mean of Hymap. Figure 4 shows the comparison of classification. Figure 4(a) shows the classification result using our improved binary encoding method, Figure 4(b) shows the ordinary binary encoding classification result using the Hymap image, Figure4(c) shows the classification result of binary encoding method on the segmented Hymap image.

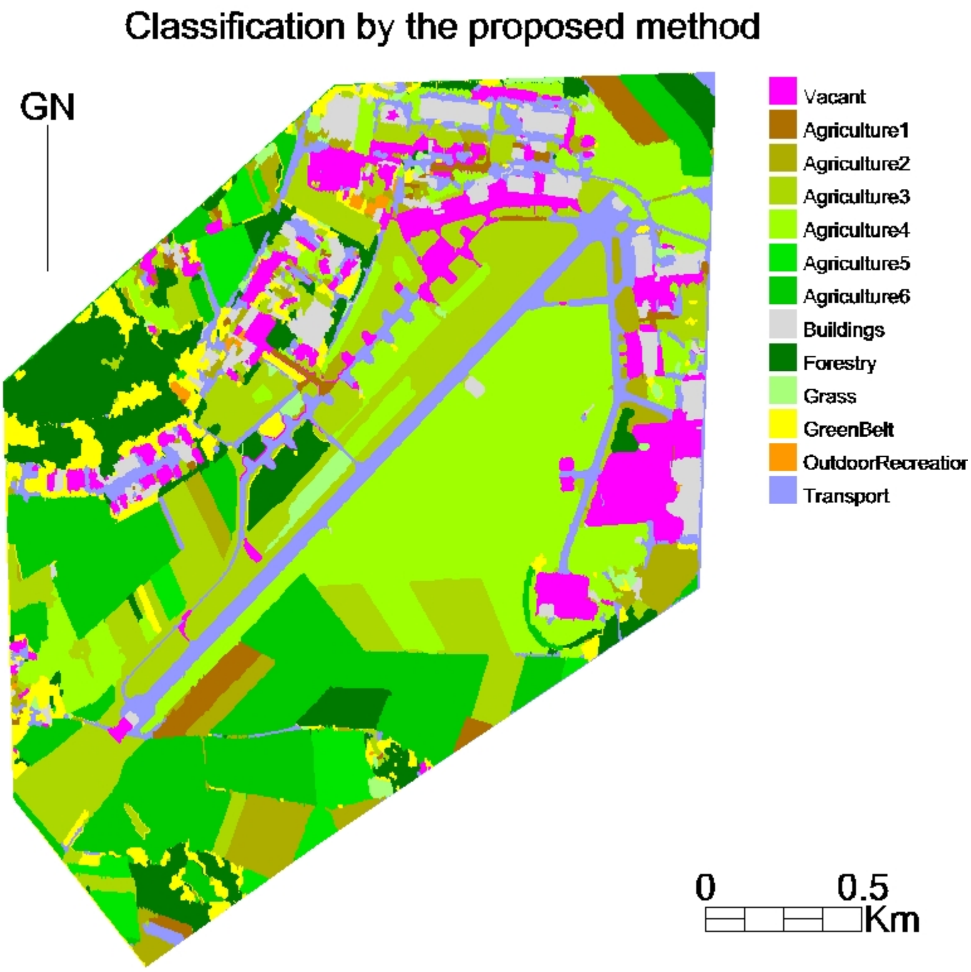

(a)

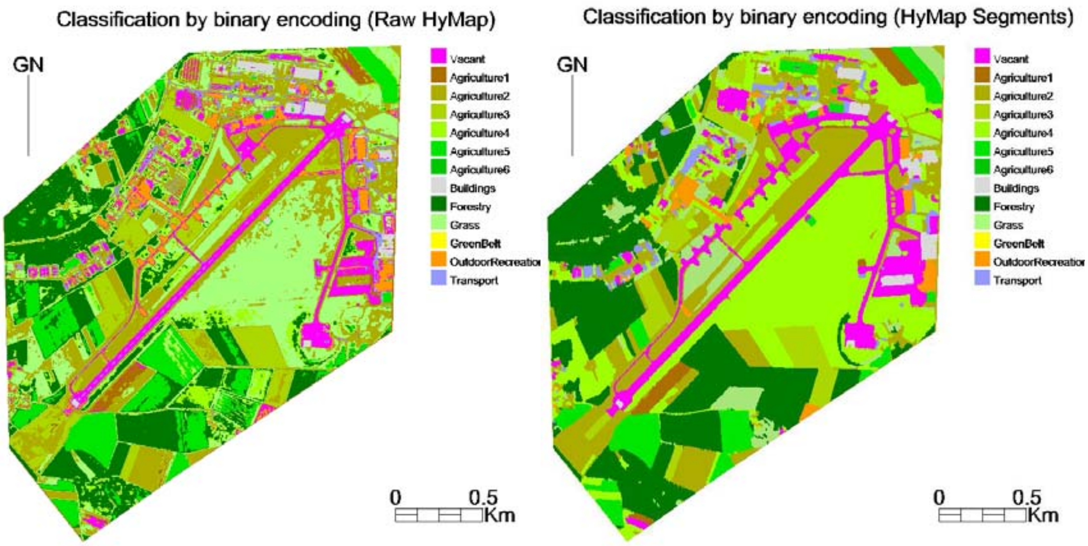

(b) (c)

Figure. 4 The classification results by binary encoding and our proposed method

From these images, we can find the biggest differences in:

1.The classification of vacant and transport

The Vacant and Transport have similar spectra but different shapes, with the help of length to width ratio, our method classified almost roads into the right class, as we can see in Figure 4(a), while Figure 4 (b) and (c) classified the roads (Blue) into vacant (Magenta),

2.The classification of buildings

Due to the various roof materials of buildings, in classification of (b) and (c), buildings were classified to other classes with similar spectra, e.g. vacant, agriculture, outdoor recreation. With additional relative height information of segment, the classification for buildings in our method is in accordance with the objects derived from the DSM data.

4 CONCLUSIONS

Based on the idea that integrating multi-sources remote sensing data may improve the interpretation of remote sensing data, a rough improved binary encoding classification method was presented. This method changes the pixel-based classification to object (segment) based classification and added the shape and the height information of segments into the codes of the segments. The primary classification results show that our method has advantages in the classification of similar spectral objects and retains the characteristics of the ordinary binary encoding method. More analysis and discussion is necessary and will be done in further research, which will concentrate on the use of texture information, the setting of the weights of the amplitude and the slope of the spectrum, the shape descriptors and the height information. In-situ experiments will also be performed to prove the precision and accuracy of classification.

ACKNOWLEDGEMENTS

Special thanks are given to the hyperspectral research group at DLR, especially Dr. Andreas Müller and Wieke Heldens, who enabled this work by supplying the hyperspectral data and the DSM free of charge.

REFERENCES

Baatz, M., Benz. U., Dehghani, S., Heynen, M., Höltje, A., Hofmann, P., Lingenfelder, Iris., Mimler, M., Weber, M. & Willhauck G., 2004. *User Guide of eCongnition*, Germany, Definiens Imaging GMBH, pp. 110-122.

Cocks, T., Jenssen, R., Stewart, A., Wilson, I. & Shields, T. *The Hymap™ Airborne Hyperspectral Sensor: The System, Calibration and Performance; 1st EARSeL Workshop on Imaging Spectroscopy, edited by Schaepman ME, Schläpfer D and D Itten K(EARSeL, Paris)*,37-42.

Mazer, A.S., Martin, M., Lee, M., & Solomon, J.E., 1988. *Image processing software for imaging spectrometry data analysis*, Remote Sensing of Environment, 24:201-210.

Robinson, D.J., Redding, N.J., & Crisp, D.J., 2002. Implementation of a fast algorithm for segmenting SAR imagery, *Scientific and Technical Report*, Australia: Defense Science and Technology Organization.

Viterbi, A. J., & Omura, J. K., 1979. *Principles of Digital Communication and Coding*, McGraw-Hill, New York, pp. 81.